Quenching of fluorescein-conjugated lipids by antibodies

Quantitative recognition and binding of lipid-bound haptens in biomembrane models, formation of two-dimensional protein domains and molecular dynamics simulations

M. Ahlers, D. W. Grainger, J. N. Herron,* K. Lim,* H. Ringsdorf, and C. Salesse

Institut für Organische Chemie, Universität Mainz, D-6500 Mainz, Germany; *Center for Biopolymers at Interfaces, Department of Bioengineering, and Department of Pharmaceutics, University of Utah, Salt Lake City, Utah 84112 USA

ABSTRACT Three model biomembrane systems, monolayers, micelles, and vesicles, have been used to study the influence of chemical and physical variables of hapten presentation at membrane interfaces on antibody binding. Hapten recognition and binding were monitored for the anti-fluorescein monoclonal antibody 4-4-20 generated against the hapten, fluorescein, in these membrane models as a function of fluorescein-conjugated lipid architecture. Specific recognition and binding in this system are conveniently monitored by quenching of fluorescein emission upon penetration of fluorescein into the antibody's active site. Lipid structure was shown to play a large role in affecting antibody quenching. Interestingly, the observed degrees of quenching were nearly independent of the lipid membrane model studied, but directly correlated with the chemical structure of the lipids. In all cases, the antibody recognized and quenched most efficiently a lipid based on dioctadecylamine where fluorescein is attached to the headgroup via a long, flexible hydrophilic spacer. Dipalmitoyl phosphatidylethanolamine containing a fluorescein headgroup demonstrated only partial binding/quenching. Egg phosphatidylethanolamine with a fluorescein headgroup showed no susceptibility to antibody recognition, binding, or quenching. Formation of two-dimensional protein domains upon antibody binding to the fluorescein-lipids in monolayers is also presented. Chemical and physical requirements for these antibody-hapten complexes at membrane surfaces have been discussed in terms of molecular dynamics simulations based on recent crystallographic models for this antibody-hapten complex (Herron et al., 1989. *Proteins Struct. Funct. Genet.* 5:271–280).

INTRODUCTION

Molecular-level surface recognition and binding are essential features of normal cell membrane function. Generally, highly specific ligand-receptor interactions characterize recognition and binding of solubilized molecules by membrane-bound receptors. Moreover, antibody recognition of cell-surface antigenic determinants specific to individual cell types or common to sets of cell types are key components of histocompatibility and immune responses. In addition, specific recognition of cell membrane epitopes by antibodies or significant fragments of antibodies forms the basis for new targeted drug delivery strategies and immunoassays. At the level of the cell membrane, therefore, selectivity and high affinity binding are critical to cell function.

Various cell membrane models have helped characterize recognition phenomena in lipid membranes, particularly the interactions between solubilized proteins and membrane-bound binding sites (for reviews, see Ringsdorf et al., 1988; McConnell et al., 1986). In lipid monolayers, high affinity binding of antibodies to lipid-bound haptens (Uzgiris and Kornberg, 1983; Uzgiris, 1987), cholera toxin to ganglioside GM 1 (Reed et al., 1987; Ribi et al., 1988), ribonucleotide reductase to nucleolipids (Ribi et al., 1987), and streptavidin to biotin lipids (Blankenburg et al., 1989; Ahlers et al., 1989) causes these proteins to self-organize into two-dimensional crystals at the interface. Hydrolytic action of the membrane-active enzyme, phospholipase A_2, has also yielded large, curious regular-shaped protein domains in lipid monolayers as detected by fluorescence microscopy (Grainger et al., 1989, 1990). In all of these systems, specific binding of macromolecules to lipid biomembrane models simulates surface recognition processes.

The fluorescein/anti-fluorescein monoclonal antibody system is a valuable hapten-binding pair to investigate interactions of antibodies with model biomembranes. Initially, the anti-fluorescein system is particularly useful for investigating the molecular basis of antigenic specificity because monoclonal antibodies with a wide range of binding affinities (10^5–10^{10} M^{-1}) are available and an array of experimental techniques can be used to access information on binding affinities, kinetics, and thermodynamics of interaction (Kranz and Voss, 1981; Kranz et al., 1982; Herron, 1984; Herron et al.,

D. W. Grainger's present address is Department of Chemical and Biological Sciences, Oregon Graduate Institute of Science and Technology, 19600 NW Von Neumann Drive, Beaverton, OR 97006-1999, USA.

C. Salesse's present address is Centre de Recherche en Photobiophysique, Université du Québec à Trois-Rivières, Trois-Rivières, Québec, Canada.

Address correspondence to H. Ringsdorf.

Abbreviations used in this paper: CMC, critical micelle concentration; CPU, central processing unit; DNP-PE, *N*-dinitrophenyl phosphatidylethanolamine; DODA-$(EO)_4$-FITC, 1-*N,N*-dioctadecylamidocarboxy-19-(5'-fluoresceinthioureoyl)-4-carboxy-5-oxa-2,8,11,14,17-pentaoxa-nonadecane; DPPC, L-α-dipalmitoylphosphatidylcholine; DPPE-FITC, L-α-*N*-fluorescein thiocarbamoyl dipalmitoyl phosphatidylethanolamine; Egg PE-FITC, egg *N*-fluorescein thiocarbamoyl phosphatidylethanolamine; Fab, Fab fragment of the 4-4-20 antibody; Fv, variable region of the Fab fragment; Fv-DODA, Fv bound to DODA-$(EO)_4$-FITC; Fv-DPPE, Fv bound to DPPE-FITC; Fv-fluor, Fv bound to free fluorescein; MD, molecular dynamics simulations; MIPS, million instructions per second; POPC, L-α-phosphatidylcholine, β-oleoyl-γ-palmitoyl; RMS, root mean squared; XRITC, rhodamine X isothiocyanate.

0006-3495/92/09/823/16 $2.00

1986; Gibson et al., 1988). Fluorescence measurements are sensitive to the fluorophore environment, leading to novel information about hapten incorporation into the antibody binding site. Recent crystallographic detail of the Fab fragment of a particular antifluorescein idiotype (Herron et al., 1989) has demonstrated with high resolution how the fluorescein hapten is bound into the active pocket and the molecular-level interactions in this region. Moreover, the use of fluorescein as both the hapten and the fluorescent probe is ideally suited for its use as a lipid-bound antigen in model biomembrane systems due to its relatively simple covalent addition to existing synthetic and natural lipids (Petrossian et al., 1985; Struck and Pagano, 1980; Knight and Stephens, 1989). Various lipids containing fluorescein as a hydrophilic headgroup are available (Petrossian et al., 1985) and its incorporation into various model biomembrane systems is rather simple (Petrossian and Owicki, 1984) so that physicochemical factors governing the binding of fluorescein by anti-fluorescein antibodies may be systematically studied. Moreover, this antibody/fluorescein-lipid system allows direct quantification of the extent of specific binding in model membranes because, upon binding, the fluorescence of the hapten is quenched.

In this investigation, the interaction, binding, and quenching behaviors of a high binding-affinity antifluorescein antibody with fluorescein-containing lipids has been studied as a function of lipid architecture and physical nature of the interface of three different biomembrane models. Fluoresceinated lipids were incorporated into lipid monolayers, micelles, and giant vesicles. The ability of the anti-fluorescein antibody to recognize and quench the fluorescein antigen in these systems has been quantitated and compared as a function of various lipid chemistries and membrane physical structures. In addition, two-dimensional antibody domain formation as a function of fluorescein-lipid binding in lipid monolayers has been directly visualized in situ using fluorescence microscopy at the air–water interface. Molecular dynamics simulations using the known crystal structure for this same antibody Fab fragment interacting with lipid monolayers are included to complement experimental measurements. These molecular models were used to support conceptual models for differences in antibody recognition observed in experimental findings.

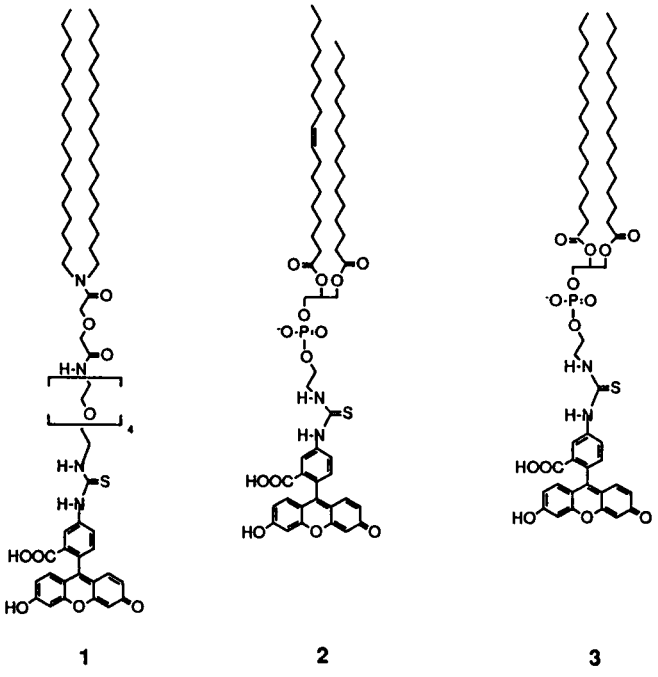

SCHEME 1 Structure of fluoresceinated lipids: (1) DODA-$(EO)_4$-FITC; (2) Egg PE-FITC; and (3) DPPE-FITC.

MATERIALS AND METHODS

L-α-dipalmitoylphosphatidylcholine (DPPC), L-α-phosphatidylcholine, β-oleoyl-γ-palmitoyl (POPC), fluorescein (sodium salt), octyl glucoside, emulphogene BC-720, and L-α-*N*-fluorescein thiocarbamoyl dipalmitoylphophatidylethanolamine (DPPE-FITC) were purchased from Sigma Chemical Co. (St. Louis, MO). DPPC and POPC were used as supplied. DPPE-FITC was reconstituted in a fresh chloroform solution by removing the solvent (chloroform-methanol) from the supplier's solution, weighing the dry product and redissolving the solid in a known amount of chloroform. 1-*N,N*-dioctadecylamidocarboxy-19-(5'-fluoresceinthioureoyl-4-carboxy-5-oxa-2,8,11,14,17-pentaoxanonadecane (DODA-$(EO)_4$-FITC) was synthesized and certified pure by NMR and fast atomic bombardment mass spectrometry as described (unpublished results). Egg phosphatidylethanolamine containing fluorescein at the head group (Egg PE-FITC) derived from hydrolysis of egg lecithin was obtained from Avanti Polar Lipids and used as supplied. All lipids were analyzed first by thin layer chromatography and then by monolayer isothermal measurements at the air–water interface (Ahlers et al., 1992). Moreover, gas chromatographic analysis of DPPE-FITC showed a fatty acid chain composition for this lipid of 96.6% 16:0 (palmitoyl), 2.4% 18:0 (stearoyl), 0.4% 18:1 (oleoyl), and 0.6% unidentified fatty acid components. The same analysis of Egg PE-FITC yielded fatty acids of the following distribution: 34.3% 16:0 (palmitoyl), 2.1% 16:1, 10.3% 18:0, 30.6% 18:1 (oleoyl), 18.1% 18:2, 0.4% 20:3w6, 2.5% 20:4w6, 0.1% 22:4w6, 0.6% 22:5w6, 0.4% 22:6w3, and 0.6% unidentified.

A 50 mM phosphate buffer (pH 8.0) and a 0.5 M sorbitol solution were prepared from high purity reagents (Merck, Darmstadt, FRG) using acid-cleaned flasks. All water was distilled three times on glass and then purified by a Milli-Q water purification system (Millipore). Its resistivity was greater than 18 MΩ-cm. Chemical structures of all fluoresceinated-lipids used in this study are shown in scheme I. The Egg PE-FITC structure is representative of the major mixed fatty acid phospholipid component (palmitoyl and oleoyl) in this compound.

A murine monoclonal antibody directed specifically against fluorescein (clone 4-4-20, anti-fluorescein antibody) was obtained from Professor Monte Reichert (Duke University) as a gift from Professor E. W. Voss, Jr. (Department of Biochemistry, University of Illinois-Champaign-Urbana). This clone is an $IgG_{2a}(\kappa)$ antibody that binds fluorescein with a binding constant of 3.4×10^{10} M^{-1} in aqueous solution (Bates et al., 1985) and shows no cross reactivity with rhodamine (Kranz and Voss, 1981; Voss et al., 1976). A portion of this monoclonal antibody was labeled with rhodamine X isothiocyanate (XRITC; Molecular Probes) using standard methods (Nargessi and Smith, 1986) and purified on a Pharmacia PD-10 (Sephadex G-50 M) column equilibrated with Millipore water. After lyophilization, the antibody product was weighed, dissolved into 50 mM phosphate buffer, pH 8.0 in Eppendorf vials, and frozen until used. The activity of both labeled and unlabeled antibodies was controlled by measuring the extent of fluores-

cence quenching of pure fluorescein in solution (phosphate buffer, pH 8.0) by a modification of the method of Petrossian and Owicki (1984). Both antibodies showed identical activities, indicating that its binding is unaffected by the labeling process.

Moreover, Scatchard analyses (data not shown) of antibody-fluorescein titrations (based on the method of Herron, 1984) yielded an antibody valency of ~2 with a binding constant of 1.9×10^9 at room temperature (23°C), which compares quite well with previously published values (Pertrossian and Owicki, 1984; Herron, 1984). This data was compared with antibody concentration data calculated from the antibody extinction coefficient from solution UV measurements. This apparent antibody concentration (8.88×10^{-7} M) was compared with that concentration determined from Scatchard analysis assuming a valency of 2 (8.5×10^{-7} M). These two values compare very well. The two approaches to assessing antibody purity and binding indicate that the antibody preparation is fully active and unaffected by labeling and subsequent handling.

Antibody recognition, binding, and fluorescence quenching in micelles

Micellar solutions of all fluorescein-lipids as well as pure fluorescein were typically prepared as follows: a 3.5×10^{-4} M solution of fluorescein-lipid was prepared by weighing the lipid with an electrobalance and solubilizing it in chloroform. Subsequently, 200 μl of this solution were withdrawn and evaporated in a 250 ml volumetric flask. This lipid was then solubilized in a 1.2×10^{-4} M solution of emulphogene in 50 mM phosphate buffer, pH 8.0, i.e., slightly above the cmc of emulphogene (8.7×10^{-5} M). Then, 200 μl of this solution were withdrawn and further diluted to 100 ml with the same emulphogene solution. Two ml of this solution, containing typically 1×10^{-12} mol of fluorescein-lipid, were then used for the fluorescence measurements. In the case of octyl glucoside, because of its much higher cmc (2.3×10^{-2} M), dilutions were performed in smaller volumes and the initial lipid concentration in chloroform was ten times more dilute. In the case of pure fluorescein, the weighed sample was solubilized and further diluted directly in the micellar (i.e., emulphogene or octyl glucoside) solution in order to reach the same final concentration as for the fluorescein-lipids. The binding constant obtained for pure fluorescein in detergent micelles is very similar to the one measured in buffer (see above).

Quenching measurements were performed by using a modification of the method of Herron (1984). Typically, 1×10^{-11} mol (50 μl) anti-fluorescein antibody was added to a 3 ml thermostatted fluorescence cuvette. Then, a quick addition of the 2 ml micellar fluorescein-lipid solution was made and the fluorescence was measured immediately. Stanton et al. (1984) have show that the excitation and emission maxima of fluorescein-lipids vary as a function of lipid hapten environment. Maximum differences between excitation maxima in several different lipid environments (e.g., DMPC/cholesterol vs. DPhPC) were 10 nm. This difference of 10 nm was witnessed also in the emission spectra. We have carefully determined the excitation and emission spectra for our haptenated lipids in micelles and compared it with free fluorescein under the same conditions. Our results show very small differences (2–3 nm shifts) in both excitation and emission spectra between the haptenated lipids. The fluorescein-lipids (and fluorescein) were thus all excited at 492 nm and their fluorescence was recorded at 522 nm. The fluorescence spectrometer used was a Spex Fluorolog equipped with a double monochromator both at the excitation and emission beams. The slits were positioned at 1.0 mm and the integration time was set at 1 s. Measurements were performed at 20°C.

Antibody recognition, binding, fluorescence quenching, and two-dimensional protein domain formation in mixed lipid monolayers

Surface pressure-area measurements

Specific binding of anti-fluorescein antibody to DODA-$(EO)_4$-FITC in mixed monolayers and its nonspecific adsorption on POPC monolayers was evaluated by measuring the expansion of monolayer molecular area at constant surface pressure. The monolayer trough used has been described previously (Albrecht, 1983). Monolayers of pure POPC or POPC containing 10 mol% DODA-$(EO)_4$-FITC were prepared by spreading ~100 μl of a 10^{-4} M lipid solution in chloroform at the air–water interface at 20°C on 50 mM phosphate buffer, pH 8.0. The film was then compressed to 16 mN/m and after 40 min equilibration time, the anti-fluorescein antibody was injected in the subphase beneath the monolayer (175 μg protein in 5 ml; subphase volume, 100 ml) and the increase in molecular area was then monitored.

Fluorescence microscopy measurements

The fluorescence microscope and the miniaturized film balance used have been described previously (Meller, 1988, 1989). For the quenching measurements, a computer-controlled high sensitivity photometer (Microscope System Processor MSP-20, Zeiss) was connected directly to the microscope photometer head via a port between the camera and the reflecting stage of the fluorescence microscope. The photometer is also equipped with a computer-controlled shutter which was set to open for 150 ms every 30 s. The POPC lipid monolayer containing 1 mol% of either DODA-$(EO)_4$-FITC, DPPE-FITC or Egg PE-FITC was prepared by spreading ~30 μl of a 4×10^{-5} M solution at the air–water interface. Solvent was allowed to evaporate and the monolayer was compressed until the desired surface pressure was reached. The 100% fluorescence intensity value was then recorded by the photometer and the anti-fluorescein antibody was injected into the subphase (15 μg in 1 ml; subphase volume, <2.5 ml) beneath the monolayer while an equivalent volume of subphase was simultaneously withdrawn from behind the compression barrier. Measurement of the decrease of monolayer fluorescence as a function of time was then immediately initiated. Additionally, in similar experiments, XRITC-labeled anti-fluorescein antibody was used to directly observe the formation of two-dimensional protein domains in fluorescein-lipid monolayers. Dual labeling (XRITC-antibody and fluorescein-lipids) allowed easy differentiation of monolayer quenching from protein domain formation. Zeiss filters 487709 and 487714 were used to visualize the fluorescein-lipids and the XRITC-labeled antibody, respectively.

As discussed above, Stanton et al. (1984) have reported that the excitation and emission maxima of fluorescein-lipids vary as a function of lipid hapten environment. However, in the present fluorescence microscopy measurements, the 487709 interferential filter used allows fluorescein excitation between 450–490 nm. The dichroic mirror used in the filter assembly has a cut-off at 510 nm and the long pass emission filter allows measurement of fluorescence above 520 nm. Moreover, the HBO100 mercury lamp on the microscope has a very flat light intensity profile in this excitation range (no lines between 450–530 nm); excitation intensity remains relatively constant across the spectrum of excitation for the various lipid hapten systems, regardless of the lipid structure, excitation maximum or environment. Moreover, the hapten lipids were consistently highly diluted (1 mol%) in the same POPC lipid environment. Possible emission shifts from environmental effects are thus accounted for by the long pass filter which detects all emission above 520 nm collectively. Red shifts in the excitation and emission bands for each hapten in the POPC matrix as a function of local hapten environment should be accounted for given the band widths of the filter system and the nature of the broad spectrum detection apparatus.

Antibody recognition, binding, and fluorescence quenching in lipid vesicle systems

Lipid mixtures containing 99 mol% DPPC and 1 mol% of either DPPE-FITC, DODA-$(EO)_4$-FITC, or Egg PE-FITC were prepared by dissolving DPPC in chloroform and adding the proper amount of each respective fluorescein-lipid in chloroform solution. Giant lipid vesicles were prepared by a procedure similar to that reported by Reeves and Dowben (1969). A volume of 5 μl of each mixture as well as a pure DPPC solution as control were deposited onto glass microscope coverslips as

small droplets. The drops were allowed to air dry and were subsequently placed in vacuum to remove residual chloroform, forming small, circular lipid films ~1 mm in diameter on the coverglass. The glass coverslips were then installed in a specially designed thermostated flow chamber (Decher et al., 1989, 1990) for observation using an inverted fluorescence microscope. The flow chamber was slowly filled with 0.5 M sorbitol solution in Millipore water and immediately heated to 45°C (above the phase transition of DPPC) to promote swelling of the lipid films into giant vesicles in the flow chamber (Servuss, 1988; Reeves and Dowben, 1969; Lasic, 1988*a*, *b*). After swelling to giant vesicles (10–100 μm diameter), the sorbitol medium in the flow chamber was exchanged slowly (0.3 ml/min flow rate) with a 50 mM phosphate buffer solution (pH 8.0) at the same temperature using a microsyringe pump. After 10 ml of buffer exchange (40 times flow chamber volume), the temperature was cooled to 37°C and allowed to equilibrate for 30 min.

XRITC-labeled anti-fluorescein antibody in the same phosphate buffer (0.1 ml, 35 μg, 2.0×10^{-9} mol) was injected slowly into the flow chamber using a microsyringe pump (flow rate 0.3 ml/min). This amount of antibody represents approximately a three-molar excess of antibody to total lipid deposited as film on the coverglass. However, such an estimation is not so valuable when considering that only a small part of the total lipid present on the glass swells into vesicles, and that only a fraction of the total lipid present as vesicles resides in the outer vesicle leaflet, exposed to antibody in the full, exterior aqueous phase. The anti-fluorescein antibody was allowed to incubate with the swollen lipid film for 30 min and excess, unbound antibody was subsequently rinsed out of the chamber with 15 ml of phosphate buffer (flow rate 0.3 ml/min).

The recognition and binding reactions of the anti-fluorescein antibody against the fluorescein hapten present as the various fluorescein-lipids in the giant vesicles was directly observed in the flow chamber using fluorescence microscopy. Giant vesicles are large enough to be easily distinguished with such methods (Ringsdorf et al., 1988; Decher et al., 1989, 1990). A Zeiss inverse IM35 microscope with phase-contrast and epifluorescence capabilities (40 times objective, working distance = 0.7 mm) has been used in combination with a reflex camera to obtain photographs of antibody binding to giant vesicles. Three types of results were sought: phase-contrast photographs of giant vesicles, photographs of the excited fluorescein-conjugated lipids in these same vesicles, and photographs of the XRITC-labeled anti-fluorescein antibody recognition and binding to these same vesicles. By switching between these various optical conditions, antibody binding to giant vesicles could be directly observed and distinguished between the various fluorescent lipid vesicles and DPPC controls. Ektachrome slide film (400 ASA) was used. 1-min exposure times were used for all XRITC-labeled anti-fluorescein antibody photographs, 30-s exposure times were used for all fluorescein-conjugated lipid photographs, and an automatic setting was used for the phase-contrast photographs. Slides were developed using standard techniques with identical developing conditions for all photographs. Prints were taken from the slides using conventional techniques. In the case of the XRITC-labeled systems where a relative quantification of antibody binding was sought by comparing fluorescence intensities, slides having the brightest XRITC fluorescence (from anti-fluorescein antibody binding to DODA-$(EO)_4$-FITC lipid vesicles) were used as the exposure standard, and all other XRITC prints were then made under these identical exposure conditions. In this way, an internally consistent method to relate XRITC intensity in each case to quantify relative antibody recognition was achieved. Each lipid vesicle experiment was repeated at least twice with the same results.

Molecular dynamics simulations of antibody interaction with lipid monolayers

Molecular simulations of the binding of fluoresceinated lipids by the 4-4-20 antibody were also performed to compare with experimental results. Complete reviews of the theory and methods of molecular simulations of biological molecules have been published (Hagler, 1985; McCammon and Harvey, 1987; Brooks et al., 1988). The computer model was constructed from three components: (*a*) the crystal structure of the variable (Fv) fragment of the 4-4-20 antibody Fab binding domain (Herron et al., 1989), (*b*) a phosphatidylcholine monolayer matrix, and (*c*) one of the three types of fluoresceinated lipids used in the experimental section (DODA-$(EO)_4$-FITC, DPPE-FITC, and Egg PE-FITC). Because of the inclusion of a large monolayer component and a limitation on computation time, only the variable region including the binding site of the Fab fragment (Fv) was included in the simulations. Total numbers of atoms numbered 1674 for the light chain of the Fv and 1834 for the heavy chain of the Fv. Three sets of 48-picosecond molecular dynamics simulations (MD) were run: (*a*) the 4-4-20 Fv bound with free fluorescein (Fv-fluor), (*b*) Fv bound to DODA-$(EO)_4$-FITC (Fv-DODA), and (*c*) Fv bound to DPPE-FITC (Fv-DPPE). In the Fv-fluor MD, energy minization of the x-ray crystal structure of bound fluorescein was performed for 100 cycles before the start of the actual MD run. The temperature of the MD was raised from 1 to 300 K in increments of 30 K/100 steps and then maintained at 300 K for the remainder of the MD run. Each step size was 1 fs. Coordinate sets of the protein-ligand system were saved every 0.1 ps or every 100 steps. The dielectric constant for the electrostatic calculations was set at 78. DISCOVER program was used in the energy minimization and MD.[1] Its performance and forcefield parameters have been published (Dauber-Osguthorpe et al., 1988; Ornstein, 1990).

In the Fv-DODA and Fv-DPPE MDs, a monolayer of phosphatidylcholine lipid structures was constructed in a planar array to simulate Fv fragments bound to the water-monolayer interface. Each phospholipid molecule was abbreviated to a C2-phosphatidylcholine form (no acyl chains) and the alkyl region of the monolayer was held fixed throughout the duration of the MD runs. For this reason, the results for DPPE-FITC are identical to those of Egg PE-FITC. 77 of these molecules were constructed and placed in a geometrical spacing similar to that known for the crystal structure of DMPC (Pearson and Pascher, 1979; Hauser et al., 1981). Energy minimization was then performed to remove steric overlaps. No periodic boundary conditions were used. A phospholipid molecule in the center of the monolayer array was then removed and replaced with the energy minimized fluoresceinated lipid of interest (DODA-$(EO)_4$-FITC or DPPE-FITC). The extended form of the fluorescein-lipid was then bound to the Fv fragment by direct superposition of fluorescein groups using the energy minimized crystal structure of Fv containing free fluorescein. Finally, the entire Fv-lipid monolayer molecular system (7196 atoms for Fv-DODA, 7161 atoms for Fv-DPPE) was subjected to molecular dynamic simulations under the same conditions as described for Fv-fluor.

Fv orientation with respect to the monolayer could not be made identical for both Fv-DODA and Fv-DPPE models. In the initial placement of the protein on the monolayer, the shorter spacer length between the fluorescein group on DPPE-FITC and the monolayer interface created a strong steric problem with the result that the Fv heavy chain resided closer to the monolayer initially in the Fv-DPPE case than in the Fv-DODA case.

To test the forcefield's ability to maintain the planarity of the fluorescein ring components, the RMS deviation of the xanthenone three-ring atoms from the plane was calculated with a subroutine from an x-ray structure refinement program, PROLSQ (Hendrickson and Konnert, 1981). The ring was placed on the x-y plane and the average displacement of the ring atoms in the z-direction was calculated. The vector perpendicular to the plane of the ring can also be calculated. The directional vectors of each of the two halves of the xanthenone were calculated and the angle between them is also used to measure the planarity of the ring. The directional vectors of the whole xanthenone and the phenyl ring were also used to calculate the angular relationship be-

[1] DISCOVER is a molecular simulation program from Biosym Technologies, San Diego, CA 92121.

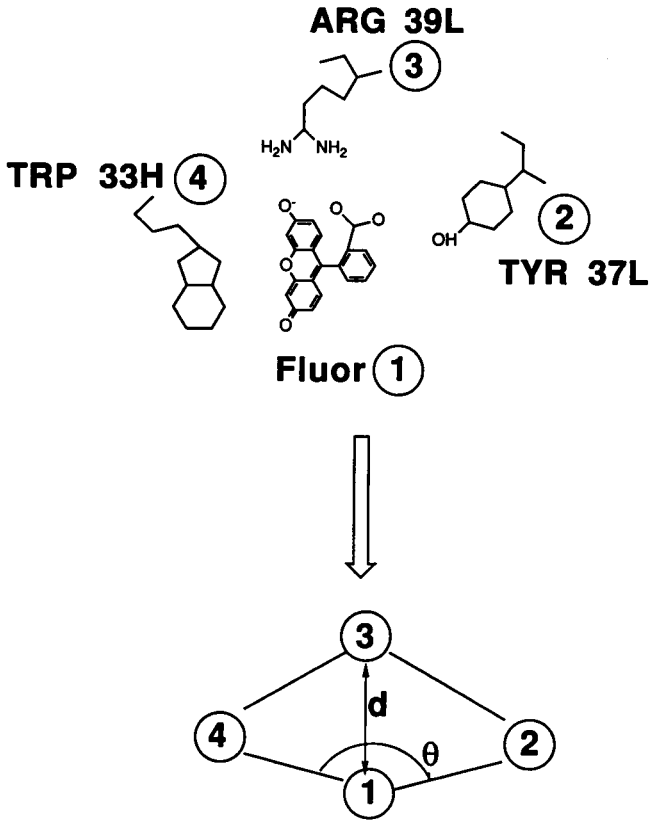

FIGURE 1 Assigned geometric relationships between the model hapten, fluorescein, and three 4-4-20 antifluorescein antibody binding site residues (ARG 39L, TRP 33H, and TYR 37L) in molecular dynamics calculations: d = distance between geometric centers of bound fluorescein and ARG39L; θ = angle formed by TRP33H, bound fluorescein, and TYR37L.

tween the two ring (xanthoyl vs. phenylcarboxy) components of fluorescein.

Also calculated were the distance, energetic, and angular relationships between bound fluorescein and certain amino acid residues in the 4-4-20 binding site (assigned geometry shown in Fig. 1). The geometrical centers for the ring portions of TYR 37L, TRP 33H, bound fluorescein, and the three atoms at the tip of the ARG 39L side chain were determined, along with the calculated distances and angles.

Fv quaternary structural changes resulting from the binding of different fluorescein conjugates were also calculated by comparing the positions of the antibody variable domain chains (V_{light} and V_{heavy}) relative to each other over time. This V_L-V_H plane angle is defined in Fig. 2 showing the angle between the Fv light and heavy chain components. The 39 C-α atoms of the conserved β-sheet residues in each of V_L and V_H domains were used to define a plane running through each domain, and then the angle between the two planes was calculated over the MD run.

RMS calculations for changes in the Cα Fv skeleton and deviation from the x-ray coordinates for certain amino acid binding site residues were also made as a function of MD run time. The changes with each hapten were referenced to an Fv-fluor structure that had been energy-minimized to less than 0.01 kcal/mol energy derivative. The final Fv-hapten complexes were superimposed upon the reference Fv-fluor structure to calculate the RMS deviations in the Cα backbone. Differences between the coordinate averages over the MD time periods were used to compare the structural changes of Fv induced with the various haptens at the monolayer interface.

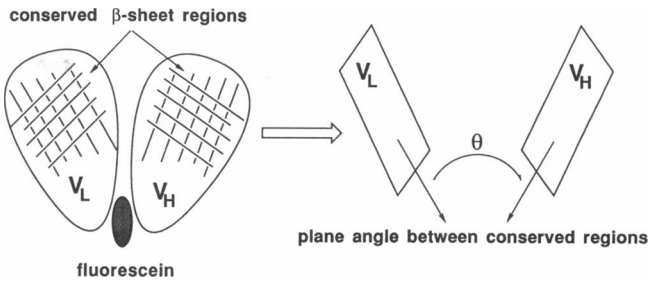

FIGURE 2 Angle defined by planes containing Cα heavy and light chain β-sheet regions in the antibody variable domains (V_L and V_H) at the terminus of each 4-4-20 Fab fragment. This angle is used to monitor changes in binding site quaternary structure upon hapten binding.

Computation of the 48-ps MD runs took 424 CPU hours on one of two processors of the Silicon Graphics 4D/220S computer rated at 20 MIPS (million instructions per second) for Fv-DODA, 448 CPU hours for Fv-DPPE and 196 CPU hours for Fv-fluor.

RESULTS

Recognition, binding, and fluorescence quenching of fluorescein-containing lipids in micelles

Fig. 3 shows the percentage of fluorescence quenching as a function of time for different fluorescein-containing lipids in micelles as compared to pure fluorescein. The kinetics observed with pure fluorescein is qualitatively faster than those obtained with the fluorescein-lipids. Moreover, pure fluorescein, DODA-$(EO)_4$-FITC, DPPE-FITC, and Egg PE-FITC show $\sim$ >90, 75, 55, and 15% fluorescence quenching in emulphogene, respectively. However, in octyl glucoside, these molecules

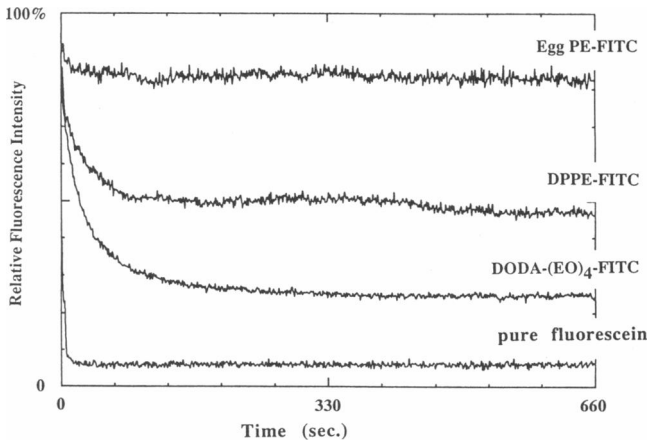

FIGURE 3 Extent of fluorescence quenching of micellar solutions of 1×10^{-12} M fluorescein-lipid (Egg PE-FITC, DPPE-FITC, or DODA-$(EO)_4$-FITC) or fluorescein by the addition of 1×10^{-11} M anti-fluorescein antibody as a function of time in 50 mM phosphate buffer, pH 8.0, containing 1.2×10^{-4} M emulphogene at 20°C.

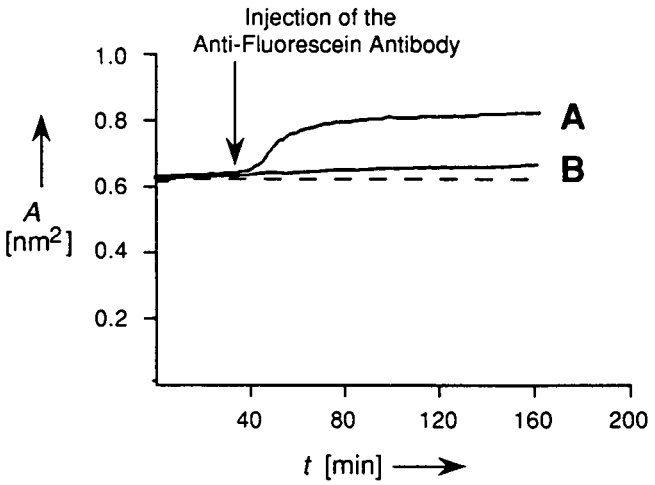

FIGURE 4 Specific binding of anti-fluorescein antibody to a mixed monolayer containing 10 mol% DODA-$(EO)_4$-FITC in 90 mol% POPC (*A*), and nonspecific adsorption of the antibody on pure POPC monolayer (*B*). The interrupted line indicates a constant surface pressure regime of 16 mN/m in the absence of antibody. Subphase is phosphate buffer (50 mM, pH 8.0, 20°C). Spreading solvent: $CHCl_3$.

show a significantly lower fluorescence quenching than that in emulphogene. Indeed, pure fluorescein, DODA-$(EO)_4$-FITC, DPPE-FITC, and Egg PE-FITC showed, respectively, 75, 55, 30, and 12% quenching (results not shown). This difference in behavior may be attributed to the much higher (250 fold) octyl glucoside:fluorescein molecule ratio (5×10^7:1) compared with that in emulphogene (2×10^5:1). In both detergents, however, the same fluorescence quenching trend is observed for all molecules: it follows a scheme where pure fluorescein > DODA-$(EO)_4$-FITC > DPPE-FITC ⋙ Egg PE-FITC. Noteworthy is that the results remained the same when twice the amount of antibody was used.

Recognition, binding, and fluorescence quenching of fluorescein-containing lipids in monolayers

Fig. 4 shows that, upon injection of the antibody beneath the POPC film containing 10 mol% of DODA-$(EO)_4$-FITC at a constant pressure of 16 mN/m, the monolayer undergoes a large expansion whereas the pure POPC film remains nearly unchanged. In fact, the DODA-$(EO)_4$-FITC/POPC monolayer molecular area was expanded by 0.2 nm^2 (20 $Å^2$/molecule) (Fig. 4). The specific binding between the anti-fluorescein antibody and DODA-$(EO)_4$-FITC can thus easily be distinguished from nonspecific adsorption even if the molar amount of this fluorescein-lipid in the POPC film is relatively small. Nonspecific adsorption of the antibody is thus very small. Very low nonspecific adsorption has also been observed in giant vesicles made of DPPC (Fig. 8 *L*).

Fig. 5 shows that a very similar trend for the fluorescence quenching behavior of the different fluorescein-lipids by the antibody is observed in monolayers as in the case of micelles. Indeed, the quenching varies from ~70% for DODA-$(EO)_4$-FITC, to ~50% for DPPE-FITC, and to ~10% for Egg PE-FITC at 30 mN/m. Larger amounts of protein did not lead to any change in these values. These absolute values are also very similar to those obtained in the fluorescence quenching experiments in emulphogene micelles (see Fig. 3). Measurements have also been performed at 5 and 12 mN/m for DODA-$(EO)_4$-FITC only (Fig. 6). In these cases, the fluorescence quenching obtained is very similar to that at 30 mN/m except that the curves contain many more fluctuations where, during several minutes, no fluorescence could be detected. Observation of these films with video microscopy after the quenching experiments showed the presence of large, round black aggregates surrounded by a homogeneous fluorescent film at surface pressures of 5 and 12 mN/m (Fig. 7). Measurements with the XRITC-labeled antibody show that these black domains observed with the fluorescein filter were fluorescent when excited by the sulforhodamine filter (Fig. 7). This indicates directly that the dark aggregates are large multimolecular clusters of XRITC-labeled antibodies bound to quenched fluorescein-lipids at the monolayer interface. No domains of any kind were observed without

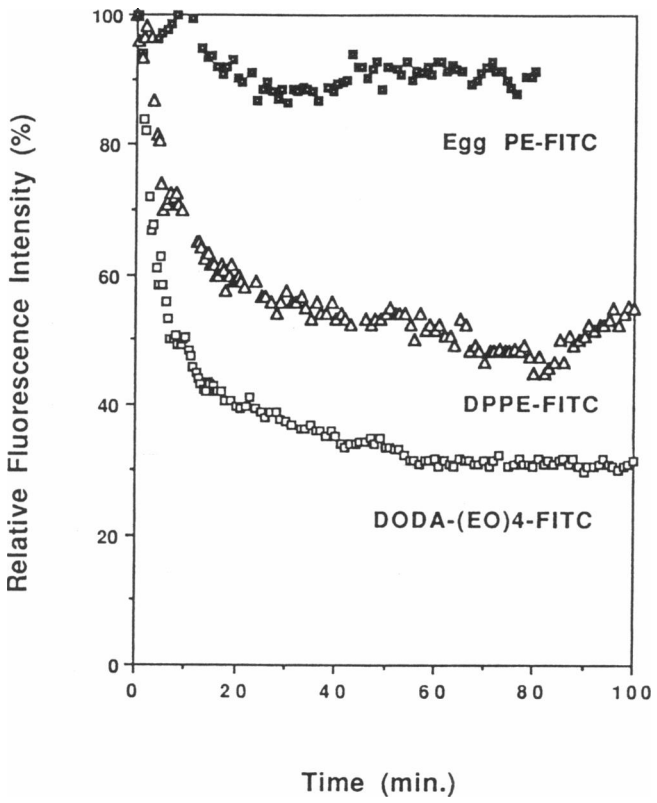

FIGURE 5 Extent of fluorescence quenching of mixed monolayers containing 1 mol% DODA-$(EO)_4$-FITC, DPPE-FITC, or Egg PE-FITC in 99 mol% POPC at 30 mN/m by the anti-fluorescein antibody. Subphase is phosphate buffer (50 mM, pH 8.0, 20°C). Spreading solvent: $CHCl_3$.

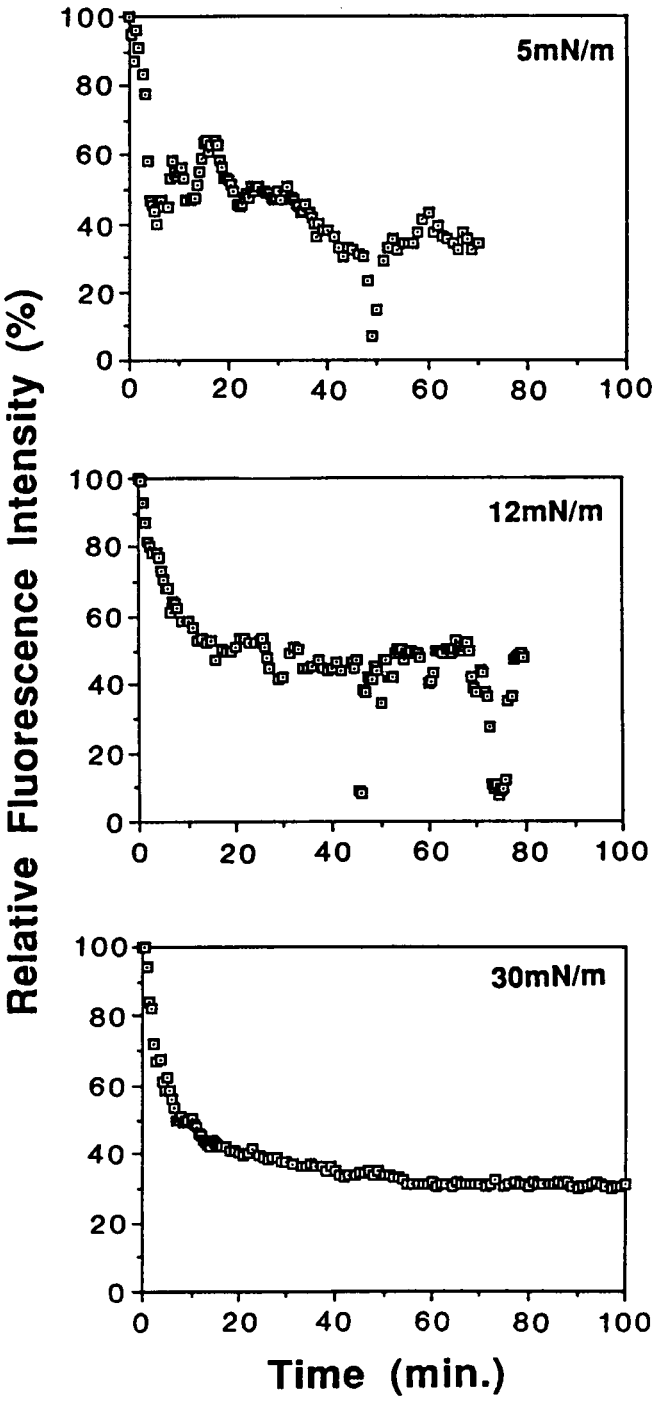

FIGURE 6 Extent of fluorescence quenching of mixed monolayers of 1 mol% DODA-$(EO)_4$-FITC in 99 mol% POPC at constant surface pressures of 5, 12, and 30 mN/m by the anti-fluorescein antibody. Other conditions as in Fig. 5.

antibody additions; phase separation and self-quenching of fluorescent lipid is not observed without antibody present (data not shown). Moreover, these antibody/lipid domains were not observed at surface pressures of 30 mN/m (figure not shown), explaining the origin of the smooth curve observed at this surface pressure (Fig. 5). Binding of both Fab fragments simultaneously to fluorescein-lipids may not be necessary to form two-dimensional protein domains, although the exact binding stoichiometry at the air–water interface is difficult to ascertain. Measurements at lower surface pressures (5 and 12 mN/m) were not performed with DPPE-FITC. However, a similar behavior could be expected for this lipid because the antibody readily binds and quenches its fluorescence although to a lesser extent than DODA-$(EO)_4$-FITC.

Recognition and binding of fluorescein-containing lipids in giant vesicles

Lipid bilayers, such as those present in vesicle systems, present a different aggregated lipid state than either the monolayer or micellar systems. Lipid motion and especially exchange (leaflet flip-flop or intervesicularly) is not as dynamic as in detergent micellar systems, and vesicles obviously maintain an element of curvature not found in the monolayer system. Moreover, quantitation of fluorescein hapten recognition and quenching is complicated by bilayer leaflets: the outer leaflet exposed to extra-vesicular aqueous medium is accessible to the antibody, whereas the inner leaflet, exposed only to the captured aqueous volume inside each vesicle is not. Quenching of fluorescence occurs, therefore, only on the outer leaflet, and can approach a value of ~65% (Petrossian and Owicki, 1984). Given a relatively low radius of curvature for giant vesicles and, therefore, a fairly homogeneous distribution of fluoresceinated lipids between both the inner and outer leaflets, quenching of fluorescein-lipids on the outer membrane leaflet cannot be visually distinguished from fluorescence emission from the unquenched inner leaflet using direct fluorescence observation of giant vesicles in a flow cell as described. To detect antibody recognition, therefore, the XRITC-labeled antibody was used for binding studies. Examination of the field alternating between a fluorescein filter and a sulforhodamine filter could then distinguish antibody's recognition and binding to the various haptenated vesicles.

Fig. 8 shows photographic evidence of antibody binding and recognition in giant lipid vesicles swollen from lipid films in a flow chamber. The first column of photos (Fig. 8, *A, D, G, J*) are phase-contrast views of swollen, giant vesicles in the flow chamber for each lipid mixture (see figure legend). The second column of photographs (Fig. 8, *B, E, H, K*) shows the same fields excited with a mercury vapor lamp and a conventional fluorescein dichroic filter system. Vesicles are seen to fluoresce bright green with homogeneous intensity (nonvesicularized solid lipid film is also seen to fluoresce under or next to some vesicles). Vesicles from DPPC as control have no intrinsic fluorescence, and the field appears homogeneously dark (Fig. 8 *K*). The third column of photo-

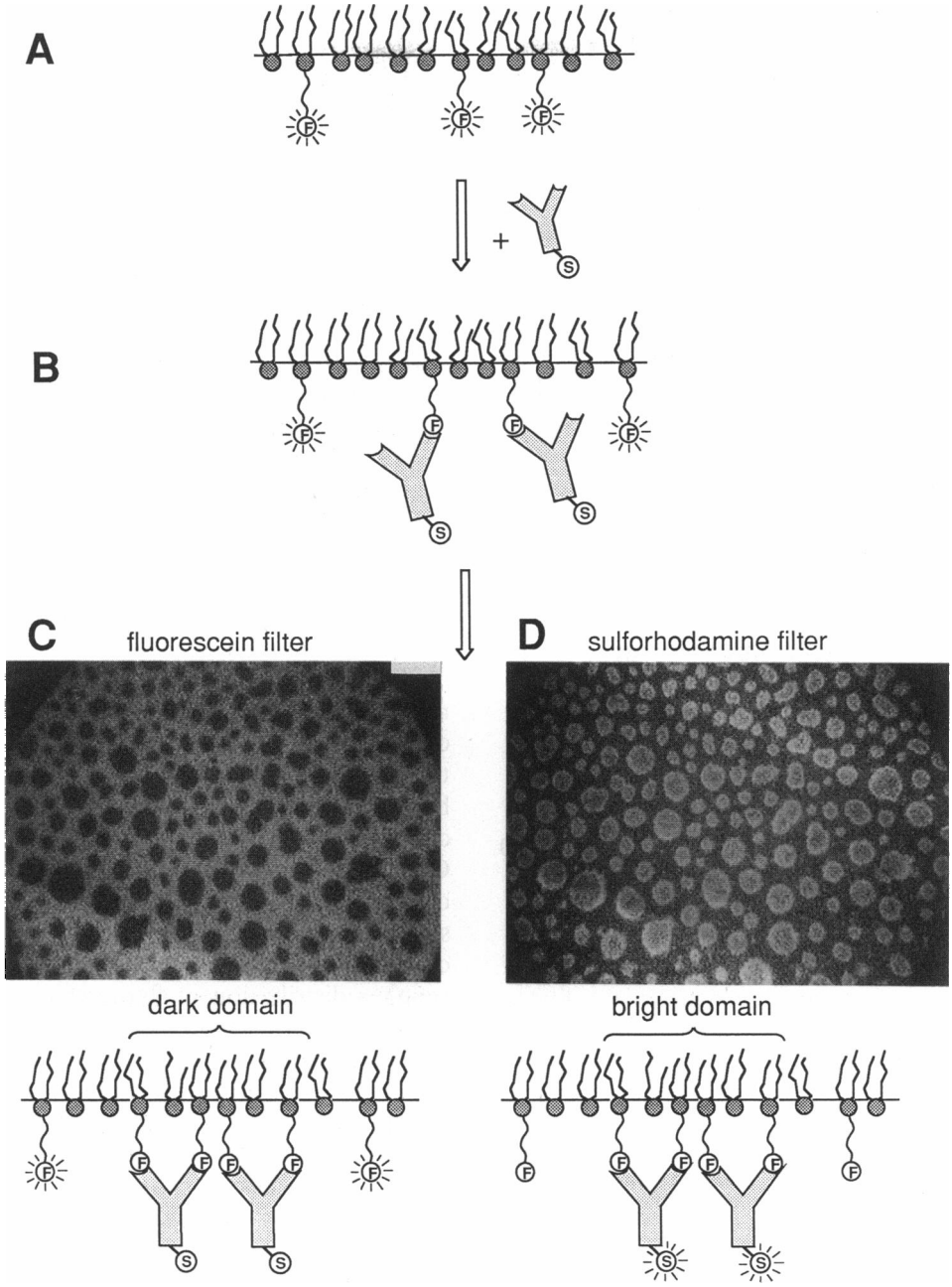

FIGURE 7 Mechanism postulated for formation of two dimensional protein domains at the lipid-water interface: (*A*) Injection of XRITC-labeled antibody beneath a monolayer of 1 mol% DODA-$(EO)_4$-FITC in 99 mol% POPC at 12 mN/m and 20°C. (*B*) Binding of the anti-fluorescein monoclonal antibody to the fluorescein-lipids and quenching of the hapten fluorescence. (*C*) By diffusion in the plane of the monolayer, the anti-fluorescein antibody/DODA-$(EO)_4$-FITC complex forms two-dimensional protein domains as observed by fluorescence microscopy of the monolayer interface. Scale bar is 20 μm. The micrograph on the left-hand side is taken using a fluorescein filter (monolayer signal of the quenched, bound fluorescein-lipids within the fluorescent DODA-$(EO)_4$-FITC (unbound)/POPC mixture); the one on the right-hand side using a sulforhodamine filter (XRITC-labeled antibody signal).

graphs (Fig. 8 *C, F, I, L*) shows the identical set of fields again, viewed under the sulforhodamine dichroic filter. Vesicles are seen to be covered to varying degrees with XRITC-labeled antibody, indicating different degrees of hapten recognition with each lipid system. Significantly, the relative degrees of antibody recognition in this vesicle system agree very well qualitatively with the above mentioned quantitative binding assessments of the antibody against monolayer and micellar systems. Vesicles containing the DODA-$(EO)_4$-FITC lipid (Fig. 8 *C*) are shown to bind the most to XRITC-labeled antibody (greatest fluorescence intensity), just as witnessed in monolayers and micelles. Vesicles of DPPE-FITC (Fig. 8 *F*) show intermediate fluorescence intensity (that is, less XRITC-labeled antibody is bound on these vesicles than on DODA-$(EO)_4$-FITC containing vesicles, but obvi-

ously more than either DPPC control or Egg PE-FITC vesicles) (Fig. 8, *L, I*). Fig. 8, (photographs *I* and *L*) shows that very little anti-fluorescein antibody is bound to vesicles containing Egg PE-FITC or DPPC, respectively, indicating that the fluorescein hapten is not recognized in the Egg PE-FITC system, and that little nonspecific binding of antibody occurs in agreement with the pure POPC monolayer measurement (Fig. 4). These results agree both in qualitative and relative quantitative terms with results for antibody recognition in monolayer and micellar lipid systems. However, different from the fluorescence microscopy observations (Fig. 7), any domain formation or patching present is neither readily observable nor distinguishable in giant vesicles but has been shown in a similar system using the identical experimental set-up (Decher et al., 1990).

Molecular dynamics of antibody bound to lipid monolayers

The molecular dynamics simulations assume that complete binding has occurred between Fv and fluorescein hapten at the start of the MD run. Based on the initial coordinates of binding in the binding site, fluorescein and Fv structures are allowed to relax within the constraints of the forcefield approximations. Data drawn from these simulations include: (*a*) distance-time, angle-time and energy-time dependencies between amino acid residues in the binding pocket and the fluorescein hapten (interactive changes in fluorescein binding), (*b*) calculation of the dynamic ring planarity of fluorescein and changes in the intramolecular angle defined by the plane of fluorescein's xanthenone ring and the plane of its phenylcarboxy ring over time, and (*c*) quaternary structural changes between heavy and light chains in the antibody variable domain as well as specific amino acids within the binding site that are indicative of conformational changes (entropic effects) of hapten binding.

Calculations for the planarity of fluorescein were intended as one validation of the forcefield model employed in these computations. If the forcefield parameters are valid, the structural integrity of fluorescein (i.e., the planar configuration of the fluorescein xanthenone) should be maintained. Indeed, the 48 ps study (data not shown) indicates an angle formed by the two perpendicular vectors of each xanthenone half ring of 174 ± 4 degrees (nearly coplanar) with an RMS deviation of 0.112 ± 0.044 Å. The angle formed by the plane of the xanthenone and the phenylcarboxy ring of fluorescein is relatively constant, fluctuating little in all cases of free fluorescein and fluorescein lipid-antibody binding (83 ± 6 degrees facing away from the active site).

Crystallography of the Fv-fluorescein complex shows that the binding pocket is long and narrow (there is a cleft between the Fv light and heavy chains [Herron et al., 1989]). In binding fluorescein, a light chain arginine residue deep in the binding pocket (ARG39L) as well as aromatic amino acids (TYR 37L, TRP 33H) are presumed to interact strongly in this low dielectric medium with the xanthoyl ring of fluorescein. ARG39L has been implicated in quenching by forming an ion pair while ring stacking with aromatic amino acids might also be significant to quenching efficiencies (see Discussion for further details). Thus, the distance-, angular-, and energy-time relationships of these amino acid residues with fluorescein have been calculated over the duration of the 48 ps MD run. All data represent the same phenomena and have similar features yielding the same conclusions. Fig. 9 shows a comparison of the electrostatic energies versus time between fluorescein and ARG39L. The absolute magnitude of the energy values can be adjusted arbitrarily by assigning dielectric constants, so only relative comparisons are significant. All atoms of fluorescein and ARG39L have been used in this calculation and ideally, there should be a linear relationship between distance and electrostatic energy (which is indeed apparent). For all three simulations (free fluorescein, DPPE-FITC, DODA-$(EO)_4$-FITC), the mean distances (indicated as "d" in Fig. 1, data not shown) and energy values (Fig. 9) show the same patterns, but the amplitude of fluctuation is what distinguishes between them. DPPE-FITC shows increasingly highly damped behavior, particularly in the last third of the 48 ps MD run, indicating hindered motions within the binding site compared to the other cases.

Fig. 10 plots the Fv quaternary structural changes with respect to the variable light and heavy chains resulting from fluorescein binding. The absolute changes in the quaternary structures during the simulation are influenced by the ligand binding and assigned dielectric conditions; only relative differences are significant for comparison. Free fluorescein binding causes the V_L–V_H plane angle to open significantly, inducing the Fv fragment to change its conformation. For the lipid-conjugated fluoresceins, the angle fluctuates substantially but does not open. Less structural changes are seen, indicating again that these lipid haptens rigidify the binding site formed by the light and heavy chains when fully bound.

DISCUSSION

The anti-fluorescein antibody used in this study (4-4-20) has already been extensively characterized. Spectroscopic and binding characteristics (Bates et al., 1985), primary structure (Bedzyk et al., 1989), and three-dimensional crystal structure with fluorescein in the binding site (Gibson et al., 1988; Herron et al., 1989) are known. Binding of fluorescein in the antibody's active site is reported to both shift the wavelength of maximum absorbance of fluorescein from 493 to 506 nm and quench a maximum of 96.4% of the fluorescence emission of the hapten (Kranz et al., 1982).

With this information already available, it was appropriate to quantitate binding of fluorescent hapten not in

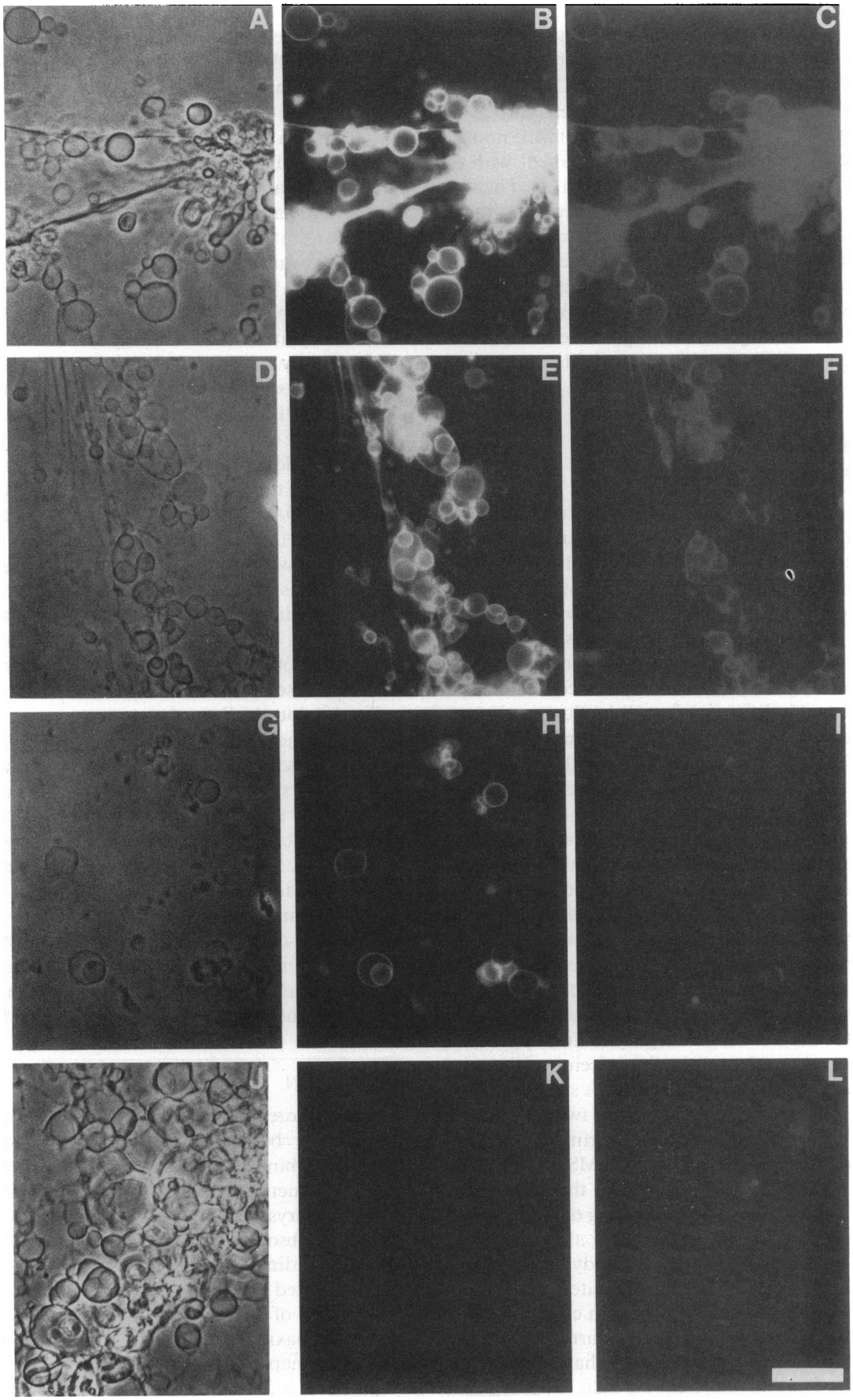
A
B
C
D
E
F
G
H
I
J
K
L

isotropic solution but as membrane-bound antigen where the architecture of various lipids as well as the differences in the interfacial physical nature of three different biomembrane models could affect the presentation of covalently-bound fluorescein to solution-phase antibody. Fluorescence methods for observing these reactions in lipid monolayers, micelles, and vesicles were thus used to quantitate surface recognition.

Among the different methods used, binding is directly visualized using fluorescence microscopy to observe fluorescence quenching of DODA-$(EO)_4$-FITC and clustering of this quenched fluorescein-lipid bound to the antibody into dark domains surrounded by homogeneous fluorescence (Fig. 7). The formation of those domains originates in the binding of the antibody to DODA-$(EO)_4$-FITC followed by the diffusion of this lipid-protein complex in the plane of the monolayer with subsequent formation of two-dimensional protein domains. Specific binding is necessary to anchor the proteins and thus compels all bound protein to assume similar orientations in two dimensions, promoting formation of two-dimensional domains through surface diffusion of the individual lipid-protein complexes. Thus, the conclusion that specific binding takes place is supported both by the formation of dark lipid clusters (quenching of fluorescein-lipid fluorescence) and the presence of the antibody in the same clusters as evidenced by the fluorescence of the XRITC-labeled antibody (Fig. 7). Possible phase separation of DODA-$(EO)_4$-FITC has been ruled out both by measuring its miscibility with POPC in monolayers and by observing the behavior of this lipid film mixture upon compression in absence of antibody by fluorescence microscopy. Indeed, high miscibility of POPC and DODA-$(EO)_4$-FITC has been shown by measuring surface pressure isotherms of mixtures of these compounds at several molar ratios. An increase of the surface pressure of DODA-$(EO)_4$-FITC phase transition as a function of POPC molar ratio was observed. This criteria has been shown to indicate high miscibility of the compounds (Cadenhead, 1985). Moreover, by fluorescence microscopy, a homogeneous bright microscope field without dark domains has been observed for POPC and DODA-$(EO)_4$-FITC mixtures. Both methods have thus shown that these compounds are highly miscible (unpublished results).

It is highly probable that POPC molecules are also included in those dark domains as a mixture with DODA-$(EO)_4$-FITC since the molecular area of each bound individual antibody (~7,000 Å^2/molecule; Uzgiris and Kornberg, 1983) is much larger than that of DODA-$(EO)_4$-FITC (~130 Å^2/molecule at 12 mN/m; unpublished results). Thus, in any given protein domain, the molecular area of each bound antibody can be accommodated by at least one bound DODA-$(EO)_4$-FITC molecule (considering partial saturation of the antibody) and approximately 100 POPC molecules (67 Å^2/molecule; unpublished results). It is uncertain whether the original 1 mol% DODA-$(EO)_4$-FITC ratio in the POPC matrix is conserved within the lipid clusters but, obviously, there is enough room to accomodate such a lipid mixture.

Such protein domains have already been observed by fluorescence microscopy in the case of streptavidin bound specifically to biotin lipid monolayers (Blankenburg et al., 1989) and those have been shown to be crystalline (Ahlers et al., 1989; Darst et al., 1991). Moreover, using a very similar system, Uzgiris and Kornberg (1983) have found that monoclonal anti-dinitrophenyl antibodies formed two-dimensional crystals upon specific binding to DNP-PE monolayers. The protein domains observed in the present study may also be crystalline but electron diffraction measurements are necessary to assess this question. Even though the high resolution three dimensional structure of the Fab fragment of this antibody is already known (Herron et al., 1989), further detailed structural electron diffraction measurements might provide new information with regard to relative antibody-membrane positional and spatial determinants and the disposition of antibody Fab and Fc fragments in both bound and unbound states.

Quantitative binding monitored by fluorescence quenching measurements of the different fluorescein-lipids both in emulphogene micelles and monolayers show surprisingly the same trend and nearly the same relative quenching differences between lipids. These two model membrane systems have very different properties. The orientation of the compounds, the lateral pressure in both systems, and their respective diffusion or exchange rates are very different. The micellar system has an extremely mobile surface due to the rapid exchange of the detergent molecules between the different micelles. This fact increases the probabilities that the antibody could bind all hapten-containing molecules present in this dynamic milieu. It can thus be hypothesized that the organization of the monolayer film does not hinder complete binding between the fluorescein-lipids and the antibody since lipids show similar fluorescence quenching both in monolayers and emulphogene micelles and more qualitatively in giant vesicles.

The primary question becomes, "what is the basis for different degrees of antibody recognition and fluorescence quenching seen in the various lipids in the three

FIGURE 8 Phase contrast (*A, D, G, J*), fluorescein filter (*B, E, H, K*), and sulforhodamine filter (*C, F, I, L*) micrographs of XRITC-labeled anti-fluorescein antibody binding to giant vesicles of either 1 mol% DODA-$(EO)_4$-FITC (*A, B, C*), DPPE-FITC (*D, E, F*), Egg PE-FITC (*G, H, I*) in 99 mol% DPPC, or pure DPPC vesicles (*J, K, L*). Flow cell and conditions are detailed in text. Scale bar = 30 μm.

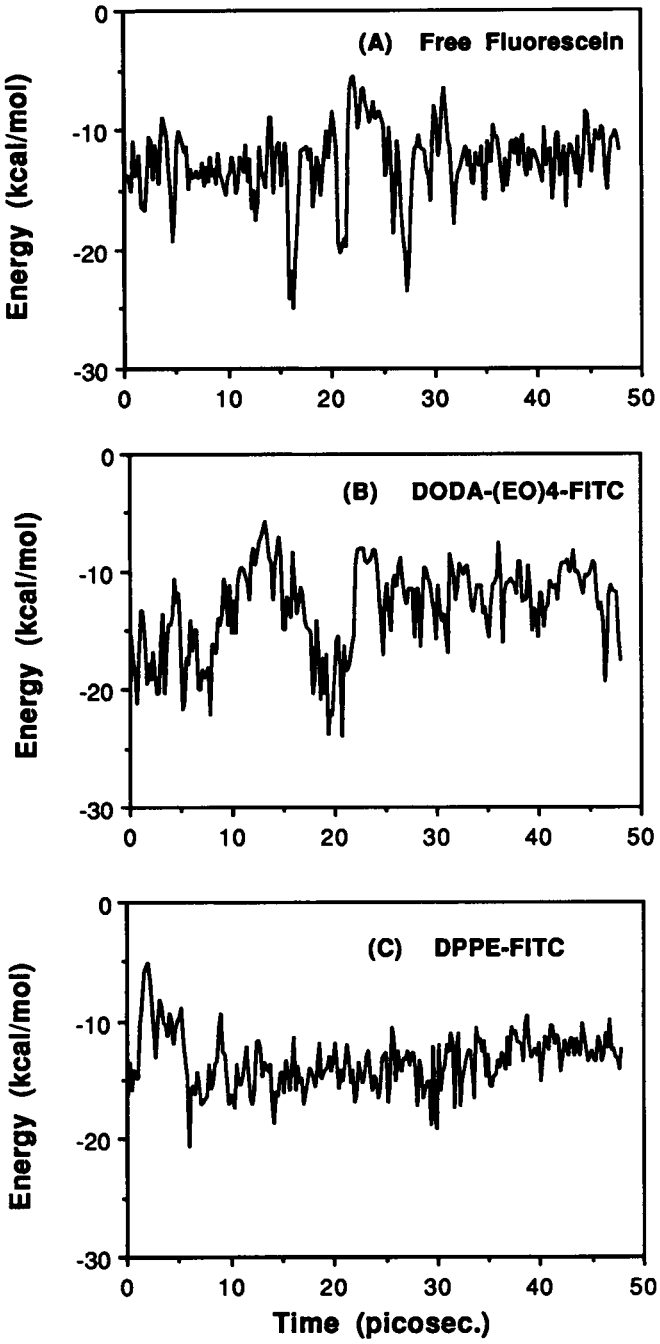

FIGURE 9 Molecular dynamics simulations results monitoring the electrostatic energy between ARG39L in the antibody binding site and fluorescein over the duration of a 48-picosecond molecular dynamics run. See text for further details of molecular dynamics model: (*A*) anti-fluorescein antibody Fv fragment bound to free fluorescein, (*B*) anti-fluorescein antibody Fv fragment bound to DODA-$(EO)_4$-FITC lipid at a lipid monolayer interface, (*C*) anti-fluorescein antibody Fv fragment bound to DPPE-FITC lipid at a lipid monolayer interface. See Fig. 1 for model geometry.

model membrane systems?". While differing lipid structures appear to be integrally involved in the answer, justification is not straightforward. Five different prototype antifluorescyl antibodies have been characterized in their ability to bind and quench fluorescein (Bates et al., 1985). Interestingly enough, widely different degrees of quenching and binding constants were found, despite high amino-acid sequence homologies (most amino-acid differences are found on the third hypervariable loop). However, all sister antibodies to the 4-4-20 prototype show lower quenching efficiencies and have a histidine residue on the light chain (position 39), whereas 4-4-20 antibody has an arginine residue at the 39th position (ARG 39L) instead. Crystallographic analysis (Herron et al., 1989; Gibson et al., 1988) of the Fab fragment of 4-4-20 antibody has recently shown that formation of an enol-arginine ion pair between enolic group on fluorescein xanthoyl ring and ARG 39L in low dielectric medium deep in the binding pocket of the antibody may account for the 2–3 orders of magnitude increase in binding affinity of the 4-4-20 molecule relative to the other members of the idiotypic anti-fluorescein family. Not only is ARG 39L critical for high affinity binding, but its position deep in the interior of the protein in an environment of low dielectric constant ensures that fluorescein must penetrate deep into the active site to be fully bound. Although unelucidated, this interaction may be critical to the higher degrees of quenching seen also for 4-4-20 antibody compared with the other sister bodies. With ARG 39L present, 4-4-20 antibodies quench up to 96.4% of fluorescence emission. Antibodies having histidine 39 substituted here show less than 60% quenching.

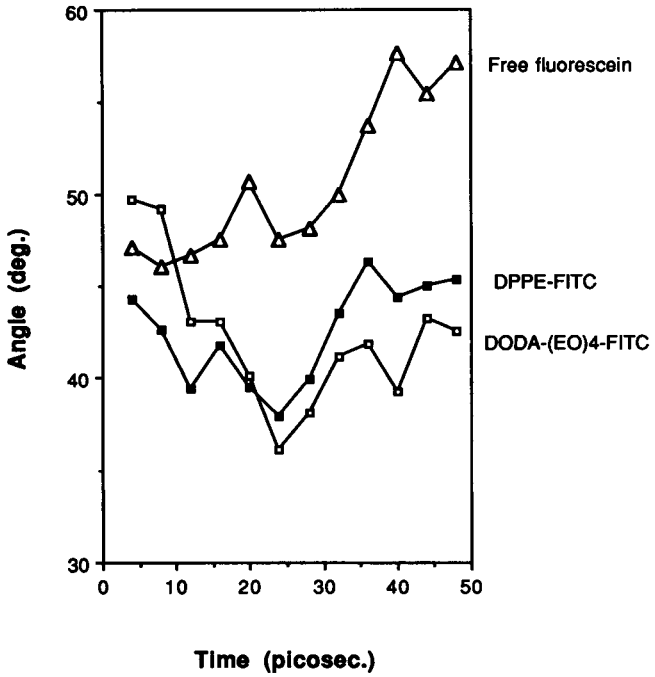

FIGURE 10 Fluctuations in the angle defined by intersecting planes containing the Cα backbone β-sheet structure of the antibody variable heavy (V_H) and variable light (V_L) chain domains as a function of fluorescein binding in the various models. See Fig. 2.

We therefore turned to computational techniques to assist in our experimental interpretations as well as in designing new experiments. One goal is to distinguish antibody binding or partial binding from fluorescence quenching (attributed only to full binding). Evidence from others (Herron et al., 1989; Berlman, 1970) supports three probable quenching mechanisms of fluorescein in the antibody binding cleft: (*a*) ring stacking between various aromatic amino acid residues lining the binding site and fluorescein, (*b*) changes in the intramolecular angle defined by the plane of fluorescein's xanthenone ring and the plane of its phenylcarboxy ring, and (*c*) delocalization of π electrons on fluorescein's xanthenone ring by ionic complexation between fluorescein enolate moieties and histidine and/or arginine residues in the binding site. By contrast, fluorescein binding is thermodynamically driven and may be independent of any electronic quenching events between fluorescein and the antibody binding site, particularly if binding is not complete or compromised by hapten structure (Swindelhurst and Voss, 1991).

Our MD data demonstrate that ring stacking is greatest in the model containing free fluorescein. The angular data (not shown) evidences more quenching interactions (possible fluorescein alignment with TYR37L and TRP 33H, and ring stacking) for free fluorescein than for DPPE-FITC and DODA-$(EO)_4$-FITC. Reduced binding site fluctuations indicated from both distance-time and V_H-V_L plane angle data could lead to reduced ring stacking in constrained systems like DPPE-FITC. Overall, the binding site for free fluorescein remains larger than that for either lipid as defined by different combinations of distances and angles for this binding site geometry. This supports both the experimental evidence on extents of quenching as well as our contention that lipid-bound haptens rigidify the binding site. That this results in reduced binding is addressed below. Additionally, intramolecular ring angles between phenyl and xanthenone fluorescein components remain similar in all three cases of simulated fluorescein binding, despite differences in spacer architecture of the lipids. This indicates, at least on the MD scale, that contributions from this quenching mechanism are identical in all cases and cannot distinguish our experiments. Charge-charge interactions between fluorescein's enolate and ARG39L are most favorable for DPPE-FITC, but both binding site and fluorescein mobility become highly damped in this case, yielding negative entropic contributions which might not be realistic as they result in structural changes in the Fv in this case (Fig. 10 and unpublished data).

The fact that both the distance and energy values as well as the angle between the two ring components of fluorescein are approximately equal for all three types of fluorescein haptens leads us to believe that the quenching mechanism is similar in these different systems with the possible exception of various modes of ring stacking. Hapten binding then becomes the primary determinant for different extents of quenching. The much reduced quenching in DPPE-FITC and somewhat reduced quenching in DODA-FITC lipids could then be due simply to reduced binding capabilities, and not from different quenching mechanisms. In fact, fluorescence intensity from micellar solutions of each hapten at very similar concentrations are in close agreement, indicating that quantum yields are very comparable in all systems. Assuming identical quenching mechanisms, binding and not quenching gives different quenching yields in each case. This leads to the question of binding site adaptability which we have addressed through structural fluctuations and mobility.

We set up the MD runs with the fully bound lipid-antibody state. The question in the simulation is how the binding site changes after some molecular dynamics. Since our results show that the average values of each parameter mentioned above are similar but the degree of fluctuation is different, the conclusion from the simulations is that the reduced quenching of DPPE (and DODA-FITC to an extent) is due to reduced binding, which in turn is due to loss of binding site mobility, configurational freedom, and entropy upon full binding. Damping of motional freedom within the binding site causes conformational changes not only in the binding site itself but also in the quaternary structure of the antibody (Fig. 10). In order for binding to occur, entropic losses from binding must be overcome. Loss of optimum binding conformation in turn induces increases in enthalpy. Support for this comes from previous thermodynamic studies (Herron et al., 1986) which showed negative heat capacities attributed largely to hydrophobic effects of hapten binding in 4-4-20 antibody for free fluorescein. Negative entropic contributions observed in these studies were attributed to restrained vibrational contributions and conformational changes upon hapten binding.

This leads us to believe that the 70% quenching seen in experiments with the DODA lipid might be further increased if the spacer length is increased. It appears that fluorescein and the binding pocket must both be allowed to move freely to achieve maximum quenching. When fluorescein binds, it must allow a certain amount of mobility for itself and for the interacting amino acid residues in the binding site. Otherwise, the rigid binding site cannot accommodate or maintain stable ligand binding. This rationale may also be extended to explain why egg-PE shows so little quenching.

When considering lipid architecture, it appears essential that the covalently conjugated fluorescein hapten be able to penetrate the binding site sufficiently close to ARG39L to form a salt bridge with an enolic oxygen of fluorescein's xanthene ring. Insufficient penetration would result in only partial or even no complex formation, decreased binding affinity, and partial or no quenching. The van der Waals contact distance from position 5 (isothiocyanate position) of the benzoyl group

of fluorescein bound in the active site to the tyrosine 103 amino acid residue positioned outermost on the tip of the Fab binding site is 6.00 Å. Considering another van der Waals contact distance of 3.5 Å as the minimum approach distance between the tyrosine and a lipid head group exterior to the binding site, a minimum of 10 Å, and more likely 15 Å is needed as a spacer length to allow an immobilized, covalently attached fluorescein hapten full ability to enter the antibody active site.

The only lipid able to fulfill this requirement experimentally is DODA-$(EO)_4$-FITC. The long, hydrophilic spacer connecting fluorescein to the hydrophobic tail region of the lipid has an approximate length of 23.3 Å, based on an energy-minimized CPK model. DPPE-FITC and Egg PE-FITC are clearly lacking a spacer, as the length from the isothiocyanate of fluorescein to the phosphodiester group along the ethanolamine chain amounts to only a fraction of the needed length (6.9 Å). Moreover, a ring of positive charge surrounding the mouth of the antibody binding site (Herron et al., 1989) would tend to hinder the phosphodiester delocalized anion of DPPE-FITC and Egg PE-FITC from penetrating into the antibody active site. Indeed, the MD evidence presented here clearly show the hindered approach of the Fv fragment to bind DPPE-FITC at the monolayer interface, as well as the dramatic conformational relaxation required to accommodate such binding. Fig. 11 shows the differences in the approaches by the Fv 4-4-20 fragment to the monolayer models containing either of the fluoresceinated lipids, DODA-$(EO)_4$-FITC (Fig. 11 *A*) and DPPE-FITC (Fig. 11 *B*). It is readily apparent that DODA's long spacer (Fig. 11 *A*) allows an easy approach of the antibody to bind the fluorescein hapten without any steric interference from the monolayer interface. Connolly surface models including the antibody hydration shell (not shown) demonstrate that the long spacer of the DODA system alleviates any need for a close approach that would hinder full binding of fluorescein deep into the active site, thus permitting full quenching. Alternatively, DPPE-FITC (Fig. 11 *B*) presents the fluorescein hapten so close to the interface that, in order to gain full binding for quenching, the Fv fragment must actually penetrate the monolayer. This steric effect must cause conformational changes in the protein (as shown in Fig. 10) and disrupt monolayer packing. Electrostatic interactions from a positive protein charge around the binding site mouth and the negative phosphodiester head group on the lipids may also contribute unfavorable energetic factors to this process of recognition by preventing a full binding of the hapten deep into the binding cleft. Thus, less fluorescein in this system is quenched experimentally.

Although the spacer effect is critical, our data demonstrate that hapten presentation is affected by factors in the lipid acyl region. Petrossian and Owicki (1984) have also shown that Egg PE-FITC does not bind to the anti-fluorescein antibody in small unilamellar vesicles. Their

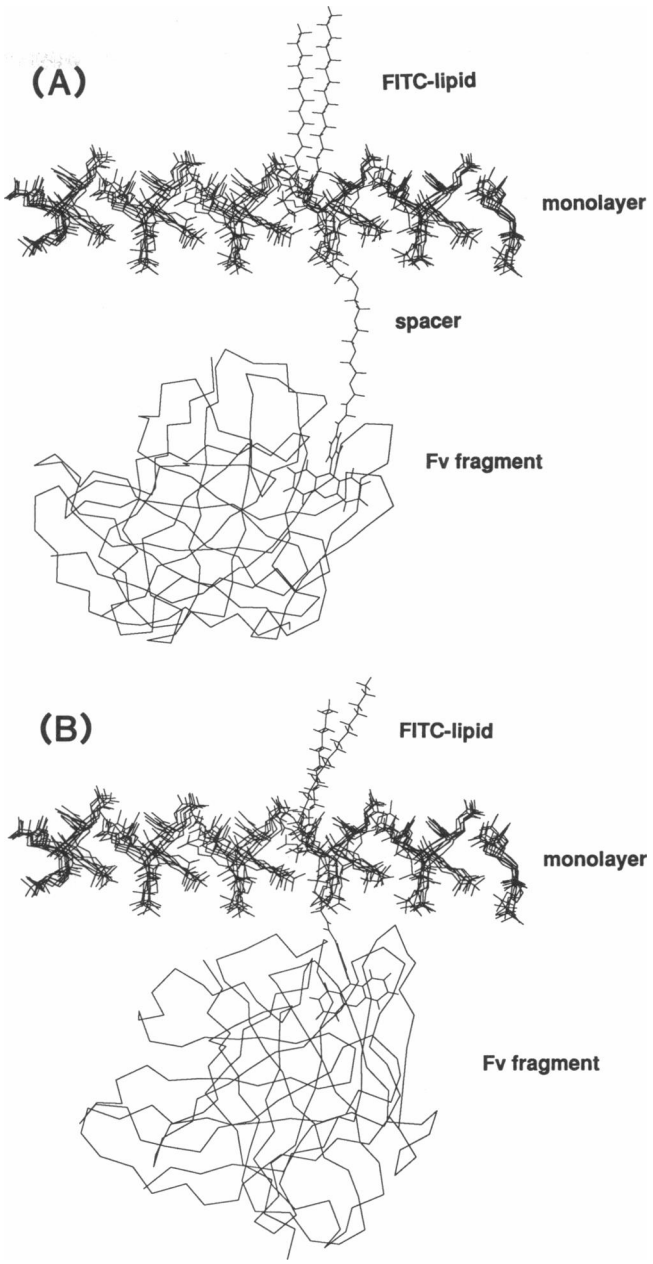

FIGURE 11 Comparisons of the Fv fragment crystal structure of the anti-fluorescein antibody fully bound to fluorescein-lipids, and energy-minimized in the molecular dynamics monolayer model. Perspective is identical in both pictures, but the scale has been changed to fill the screen with each image: (*A*) Fv-DODA$(EO)_4$-FITC complex at the model lipid monolayer interface, and (*B*) Fv-DPPE-FITC complex at the model lipid monolayer interface.

data, however, was explained by the absence of a long enough spacer between fluorescein in the head group and the fatty acid chains. The present data shows that this simple interpretation cannot account for quenching differences between these. Indeed, DPPE-FITC, which bears the same polar head group as Egg PE-FITC, shows a significant fluorescence quenching by the antibody in micelles, monolayers and giant vesicles. Therefore, another mechanism must be put forward to explain this

difference between the behavior of these two fluorescein-lipids.

Time-resolved computer modeling data based on dioleoylphosphatidylcholine indicate that unsaturated alkyl chains in phospholipids can, over very short time scales, cause phosphatidylcholine head groups to partially rescind into a loop formed by kinked and curled unsaturated alkyl chains (figure not shown). In mixed monolayers and vesicles, this could result in the fluorescein hapten being pulled away from the aqueous environment, up against the hydration shell of the aggregated lipid membrane and out of reach of the antibody. Such a conformation reduces the effective spacer length between the membrane and the hapten, virtually preventing the antibody from any binding at all. This explanation, however, does not apply to micelle systems where surfactant exchange is so rapid and aggregate surfaces are always in rapid dynamic flux. The oleoyl acyl chains must affect head group conformation and hapten presentation.

Our conclusion is, therefore, that antibody recognition, binding, and fluorescence quenching in these three model membrane systems are much more dependent on lipid architecture, in particular, the requirement of a long spacer to attach the fluorescein hapten, than on the physical structure of the biomembrane models in which the hapten is presented. However, the behavior of the bound protein depends on the physical properties of the model membrane, as shown in Fig. 6 where the mobility of the antibody-lipid complex is determined by the lateral packing within the monolayer. Fluorescence quenching, as a direct indicator of recognition, requires fluorescein to sit deep in the antibody binding site, complexed in a salt bridge with ARG 39L at the base of the binding pocket. Only spacer-containing lipids allowing the fluorescein moiety a 10–15 Å distance to enter the pocket will manifest full binding affinity and maximum quenching efficiency. In this respect, only DODA-$(EO)_4$-FITC fulfills these criteria.

Experimentally, these modeling predictions are confirmed, with the antibody able to recognize 70% of this lipid-bound hapten in monolayers, micelles, and vesicles. By contrast, 50% of DPPE-FITC could be quenched in these systems indicating some partial binding and incomplete hapten penetration. Egg PE-FITC, however, showed less than 10% quenching in monolayers, micelles, and vesicles, indicating a lipid conformation and hapten presentation completely incompatible with antibody recognition and binding. Identical head group chemistries in these two lipids prevent simple interpretation based on short spacer haptens. Acyl chain saturation affects hapten presentation at the membrane-water interface. Additional computational analyses calculating energy fluctuations and contributions to binding capacities by ring residues in the 4-4-20 active site are currently underway to clarify these differences. Partial binding of fluorescein haptens in the binding cleft is also being simulated to assess incomplete quenching and contributions from residues in the active site to accommodate full binding.

The gift of the 4-4-20 antibody from the lab of Professor E. W. Voss, Jr. (University of Illinois-Champaign-Urbana) is gratefully acknowledged. K. Lim and J. Herron thank Biosym Technologies for the generous donation of DISCOVER and INSIGHT molecular graphics programs and Silicon Graphics Inc. for the SGI 4D/70GT workstation. Discussions with Dr. Peter Suci regarding Scatchard analyses were of great assistance.

D. W. Grainger was the recipient of an Alexander von Humboldt Postdoctoral Research Fellowship (West Germany) and was partially supported through an institutional grant from the Department of Energy, Basic Energy Sciences Program. C. Salesse was supported by a postdoctoral fellowship from the Natural Sciences and Engineering Research Council of Canada. Research in Mainz was supported by a BMFT Project on Ultrathin Films. This work was partially supported by Public Health Service grant A1 22898 (to J. Herron) and the Center for Biopolymers at Interfaces, University of Utah.

Received for publication 1 April 1991 and in final form 25 February 1992.

REFERENCES

Ahlers, M., R. Blankenburg, D. W. Grainger, P. Meller, H. Ringsdorf, and C. Salesse. 1989. Specific recognition and formation of two-dimensional streptavidin domains in monolayers: applications to molecular devices. *Thin Solid Films.* 180:93–98.

Albrecht, O. 1983. The construction of a microprocessor-controlled film balance for precision measurements of isotherms and isobars. *Thin Solid Films.* 99:227–232.

Bates, R. M., D. W. Ballard, and E. W. Voss, Jr. 1985. Comparative properties of monoclonal antibodies comprising a high-affinity anti-fluorescyl idiotype family. *Mol. Immunol.* 22:871–877.

Bedzyk, W. D., L. S. Johnson, G. S. Riordan, and E. W. Voss, Jr. 1989. Comparison of variable region primary structures within an anti-fluorescein idiotype famely. *J. Biol. Chem.* 264:1565–1569.

Berlman, I. B. 1970. On an empirical correlation between nuclear conformation and certain fluorescence and absorption characteristics of aromatic compounds. *J. Phys. Chem.* 74:3085–3093.

Blankenburg, R., P. Meller, H. Ringsdorf, and C. Salesse. 1989. Interaction between biotin lipids and streptavidin in monolayers: formation of oriented two-dimensional protein domains induced by surface recognition. *Biochemistry.* 28:8214–8221.

Brooks, C. L., B. M. Karplus, and B. M. Pettit. 1988. Proteins: a theoretical perspective of dynamics, structure, and thermodynamics. *Adv. Chem. Phys.* 71:1–259.

Cadenhead, D. A. 1985. Monomolecular films as biomembrane models. *In* Structure and Properties of Cell Membranes. G. Benga, editor. Vol. III. CRC Press, Boca Raton, FL. 21–62.

Darst, S. A., M. Ahlers, P. Meller, E. W. Kubalek, R. Blankenburg, H. O. Ribi, R. D. Kornberg, and H. Ringsdorf. 1991. Two-dimensional crystals of streptavidin on biotinylated lipid layers and their interactions with biotinylated macromolecules. *Biophys. J.* 59:387–396.

Decher, G., E. Kuchinka, H. Ringsdorf, J. Venzmer, D. Bitter-Suermann, and C. Weisgerber. 1989. Interaction of amphiphilic polymers with model biomembranes. *Angew. Makromol. Chem.* 166/167:71–80.

Decher, G., H. Ringsdorf, J. Venzmer, D. Bitter-Suermann, and C. Weisgerber. 1990. Giant liposomes as model membranes for immu-

nological studies: spontaneous insertion of purified K1-antigen (poly-α-2,8-NeuAc) of *Escherichia coli*. *Biochim. Biophys. Acta.* 1023:357–364.

Dauber-Osguthorpe, P., V. A. Roberts, D. J. Osguthorpe, J. Wolff, M. Genest, and A. T. Hagler. 1988. Structure and energetics of ligand binding to proteins: *Escherichia coli* dihydrofolate reductase-trimethoprim, a drug-receptor system. *Proteins Struct. Funct. Genet.* 4:31–47.

Gibson, A. L., J. N. Herron, X.-M. He, V. A. Patrick, M. L. Mason, J.-N. Lin, D. M. Kranz, E. W. Voss, Jr., and A. B. Edmundson. 1988. Differences in crystal properties and ligand affinities of an antifluoresceyl Fab (4-4-20) in two solid systems. *Proteins Struct. Funct. Genet.* 3:155–160.

Grainger, D. W., A. Reichert, H. Ringsdorf, and C. Salesse. 1989. An enzyme caught in action: direct imaging of hydrolytic function and domain formation of phospholipase A_2 in phosphatidylcholine monolayers. *FEBS Lett.* 252:73–82.

Grainger, D. W., A. Reichert, H. Ringsdorf, and C. Salesse. 1990. Hydrolytic action of phospholipase A_2 in monolayers in the phase transition region: direct observation of enzyme domain formation using fluorescence microscopy. *Biochim. Biophys. Acta.* 1023:365–379.

Hagler, A. T. 1985. Theoretical simulation of conformation, energetics, and dynamics of peptides. *Peptides.* 7:213–299.

Hauser, H., I. Pascher, R. H. Pearson, and S. Sundell. 1981. Preferred conformation and molecular packing of phosphatidylethanolamine and phosphatidylcholine. *Biochim. Biophys. Acta.* 650:21–51.

Hendrickson, W. A., and J. H. Konnert. 1981. *In* Biomolecular Structure, Conformation, Function and Evolution. R. Srinivasan, E. Subramanian, and N. Yathindra, editors. Pergamon Press, New York. Vol. 1:43–57.

Herron, J. N. 1984. Equilibrium and kinetic methodology for the measurement of binding properties in monoclonal and polyclonal populations of antifluorescyl-IgG antibodies. *In* Fluorescein Hapten: An Immunological Probe. E. W. Voss, Jr., editor. CRC Press, Boca Raton, FL. 49–76.

Herron, J. N., W.-M. He, M. L. Mason, E. W. Voss, Jr., and A. B. Edmundson. 1989. Three-dimensional structure of a fluorescein-Fab complex crystallized in 2-methyl-2,4-pentanediol. *Proteins Struct. Funct. Genet.* 5:271–280.

Herron, J. N., D. M. Kranz, D. M. Jameson, and E. W. Voss, Jr. 1986. Thermodynamic properties of ligand binding by monoclonal antifluorescyl antibodies. *Biochemistry.* 25:4602–4609.

Knight, C. G., and T. Stephens. 1989. Xanthine/dye-labeled phosphatidylethanolamines as probes of interfacial pH. *Biochem. J.* 258:683–689.

Kranz, D. M., J. N. Herron, and E. W. Voss, Jr. 1982. Ligand binding by monoclonal and antifluorescyl antibodies. *J. Biol. Chem.* 257:6987–6995.

Kranz, D. M., and E. W. Voss, Jr. 1981. Partial elucidation of an anti-hapten repertoire in BALB/c mice: comparative characterization of several monoclonal anti-fluorescyl antibodies. *Mol. Immunol.* 18:889–898.

Lasic, D. 1988a. The mechanism of vesicle formation. *Biochem. J.* 256:1–11.

Lasic, D. 1988b. The spontaneous formation of unilamellar vesicles. *J. Colloid Interface Sci.* 124:428–435.

McCammon, J. A., and S. C. Harvey. 1987. Dynamics of Proteins and Nucleic Acids. Cambridge University Press, Cambridge, UK.

McConnell, H. M., T. H. Watts, R. M. Weis, and A. A. Brian. 1986. Supported planar membranes in studies of cell-cell recognition in the immune system. *Biochim. Biophys. Acta.* 864:95–106.

Meller, P. 1988. Computer-assisted video microscopy for the investigation of monolayers on liquid and solid substrates. *Rev. Sci. Instrum.* 59:2225–2231.

Meller, P. 1989. Microspectroscopy on single domains of phase-separated monolayers. *J. Microscopy.* 156:241–246.

Nargessi, R. D., and D. S. Smith. 1986. Fluorometric assays for avidin and biotin. *Methods Enzymol.* 122:67–72.

Ornstein, R. L. 1990. Using molecular dynamics simulations on crambin to evaluate the suitability of different continuum dielectric and hydrogen atom models for protein simulations. *J. Biomol. Struct. Dynam.* 7:1019–1041.

Pearson, R. H., and I. Pascher. 1979. The molecular structure of lecithin dihydrate. *Nature (Lond.).* 281:499–501.

Petrossian, A., A. B. Kantor, J. C. Owicki. 1985. Synthesis and characterization of a highly fluorescent peptidyl/phosphatidylethanolamine. *J. Lipid Res.* 26:767–773.

Petrossian, A., and J. C. Owicki. 1984. Interaction of antibodies with liposomes bearing fluorescent haptens. *Biochim. Biophys. Acta.* 776:217–237.

Reed, R. A., J. Mattai, and G. G. Shipley. 1987. Interaction of cholera toxin with ganglioside GM1 receptors in supported lipid monolayers. *Biochemistry.* 26:824–832.

Reeves, J. P., and R. M. Dowben. 1969. Formation and properties of thin-walled phospholipid vesicles. *J. Cell Physiol.* 73:49–60.

Ribi, H. O., D. S. Ludwig, K. Lynne Mercer, G. K. Schooinik, and R. D. Kornberg. 1988. Three-dimensional structure of cholera toxin penetrating a lipid membrane. *Science (Wash. DC).* 239:1272–1276.

Ribi, H. O., P. Reichard, and R. D. Kornberg. 1987. Two-dimensional crystals of enzyme-effector complexes: ribonucleotide reductase at 18-Å resolution. *Biochemistry.* 26:7974–7979.

Ringsdorf, H., B. Schlarb, and J. Venzmer. 1988. Molecular architecture and function of polymeric oriented systems: models for the study of organization, surface recognition and dynamics of biomembranes. *Angew. Chem. Int. Ed. Engl.* 27:113–198.

Servuss, R.-M. 1988. Spontaneous formation of giant phospholipid vesicles. *Z. Naturforsch.* 43c:938–947.

Stanton, S. G., A. B. Kantor, A. Petrossian, and J. C. Owicki. 1984. Location and dynamics of a membrane-bound fluorescent hapten. A spectroscopic study. *Biochim. Biophys. Acta.* 776:228–236.

Struck, D. K., and R. E. Pagano. 1980. Insertion of fluorescent phospholipids into the plasma membrane of a mammalian cell. *J. Biol. Chem.* 255:5404–5401.

Swindlehurst, C. A., and E. W. Voss, Jr. 1991. Fluorescence measurements of immune complexes of Mab 4-4-20 with isomeric haptens. *Biophys. J.* 59:619–628.

Uzgiris, E. E. 1987. Self-organization of IgE immunoglobulins on phospholipid films. *Biochem. J.* 242:293–296.

Uzgiris, E. E., and R. D. Kornberg. 1983. Two-dimensional crystallization technique for imaging macromolecules, with application to antigen-antibody-complement complexes. *Nature (Lond.).* 301:125–129.

Voss, E. W., Jr., W. Eschenfeldt, and R. T. Root. 1976. Fluorescein: a complete antigenic group. *Immunochemistry.* 13:447–453.